

# New High Temperature Diboride Superconductors: $\text{AgB}_2$ and $\text{AuB}_2$

S. K. Kwon<sup>1</sup>, S. J. Youn<sup>2</sup>, K. S. Kim<sup>2</sup>, and B. I. Min<sup>1</sup>

<sup>1</sup> *Department of Physics, Pohang University of Science and Technology, Pohang 790-784, Korea*

<sup>2</sup> *National Creative Research Initiative Center for Superfunctional Materials, Department of Chemistry, Pohang University of Science and Technology, Pohang 790-784, Korea*

(November 20, 2018)

Based on electronic structure calculations, we have found that noble metal diborides,  $\text{AgB}_2$  and  $\text{AuB}_2$ , are potential candidates for conventional BCS-type high temperature superconductors. B  $2p$  density of states dominates at the Fermi level in comparison with Ag  $4d$  and Au  $5d$  states. Furthermore, the electron-phonon coupling constant  $\lambda$  is much larger in  $\text{AgB}_2$  and  $\text{AuB}_2$  than in  $\text{MgB}_2$ . Estimated transition temperatures for  $\text{AgB}_2$  and  $\text{AuB}_2$  are  $T_c^{\text{cal}} = 59$  K and 72 K, respectively. These are about 2 ~ 3 times higher than the estimated  $T_c^{\text{cal}} = 27$  K in  $\text{MgB}_2$  and almost comparable to those in cuprate superconductors.

PACS number: 74.25.Jb, 74.25.Kc, 74.70.Ad, 74.20.Fg

Due to the highest transition temperature of  $T_c \simeq 39$  K [1] among nonoxide bulk metallic superconductors,  $\text{MgB}_2$  has renewed scope of the transition temperature in the conventional BCS superconductors. Photoemission spectroscopy [2], tunneling spectroscopy [3], isotope effect measurements [4,5], and inelastic neutron scattering measurements [6] support that  $\text{MgB}_2$  belongs to the  $s$ -wave phonon-mediated BCS superconductor. Borons in  $\text{MgB}_2$  can generate high frequency in-plane phonon modes caused by their light atomic masses. These phonons are thought to be responsible for the observed unusual high  $T_c$ . It is also found that electron doped  $\text{Mg}_{1-x}\text{Al}_x\text{B}_2$  loses superconductivity for  $x > 0.1$  [7]. In  $\text{MgB}_2$ , the Fermi level ( $E_F$ ) is located at the shoulder of the density of states (DOS) curve in which B  $2p$  states, believed to become superconducting carriers, are dominant. Thus, electron doping effect in  $\text{Mg}_{1-x}\text{Al}_x\text{B}_2$  would move  $E_F$  to the lower DOS side and destroy B  $2p$  hole states and superconductivity by reducing the effective electron-phonon interaction strength [8,9].

$\text{MgB}_2$  research society becomes rapidly growing and it is amazing that some significant progresses have already been made toward technological applications [10–14]. However, it is open and natural to ask how many diborides can be categorized as superconductors with  $T_c$  as high as  $\text{MgB}_2$  and what is the upper limit of the transition temperature in these BCS superconductors.

In hexagonal  $\text{AlB}_2$ -type structure,  $\text{MgB}_2$  is special with superconductivity itself even excluding high  $T_c \simeq 39$  K. Other than  $\text{MgB}_2$ , only a few diborides show superconductivity:  $\text{Zr}_{0.13}\text{Mo}_{0.87}\text{B}_2$ ,  $\text{NbB}_2$  [15], and  $\text{TaB}_2$  [16] with  $T_c \lesssim 10$  K. There are, however, still controversies for  $\text{NbB}_2$  and  $\text{TaB}_2$  [17–19]. Since the discovery of  $\text{MgB}_2$ , there have been several theoretical studies to search for the potential high  $T_c$  binary and ternary borides in isoelectronic systems such as  $\text{BeB}_2$  and  $\text{CaB}_2$ , transition metal (TM) diborides  $\text{TM}\text{B}_2$ , and hole doped systems such as  $\text{Mg}_{1-x}\text{M}_x\text{B}_2$  ( $M = \text{Li, Na, Cu, and Zn}$ ) [20–23]. However, most of the recent experimental works for related binary and ternary borides fail to find another high temperature diboride superconductor ( $\text{HT}_c\text{BS}$ ) [19,24,25]. Nevertheless, in the present work, we try to give

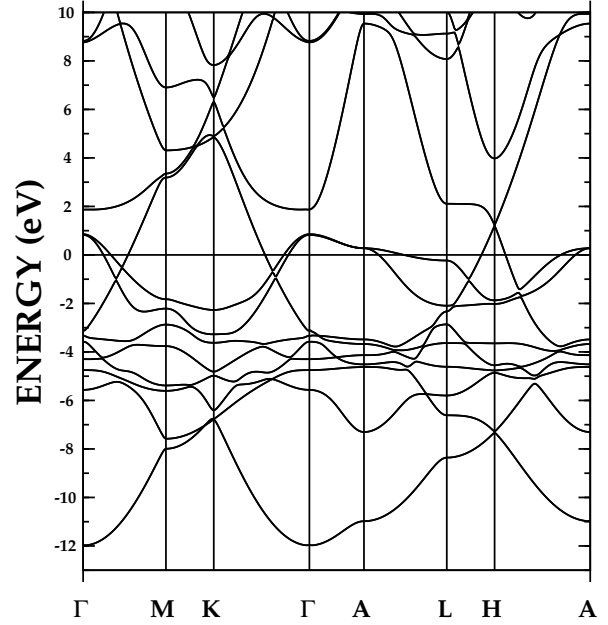


FIG. 1.  $\text{AgB}_2$  band structures along high symmetry lines. Along  $\Gamma$ -A-L lines, B  $2p_{x,y}\sigma$  hole bands are formed near  $E_F$  similarly to  $\text{MgB}_2$ .

positive answers to the given questions. We suggest that noble metal diborides,  $\text{AgB}_2$  and  $\text{AuB}_2$  which correspond to effectively hole doped systems, are potential candidates for  $\text{HT}_c\text{BS}$ . We have found that their transition temperatures are 2 ~ 3 times higher than that in  $\text{MgB}_2$ .

To verify its possibility, we have performed fully relativistic electronic structure calculations for  $\text{AgB}_2$  and  $\text{AuB}_2$  by using the linearized muffin-tin orbital (LMTO) band method. We have used lattice constants of  $a = 2.98$  Å and  $c = 3.92$  (4.05) Å for  $\text{AgB}_2$  ( $\text{AuB}_2$ ) [26]. Hence the B-B interlayer distances are much increased as compared to that in  $\text{MgB}_2$ , while the B-B in-plane bond lengths are similar. The Coulomb exchange correlation potential is treated in the von Barth-Hedin form of the local spin-density approximation. For the self-consistent charge density integration, 280  $k$ -points sampling is done in the irreducible wedge of the first Brillion zone (BZ). Basis

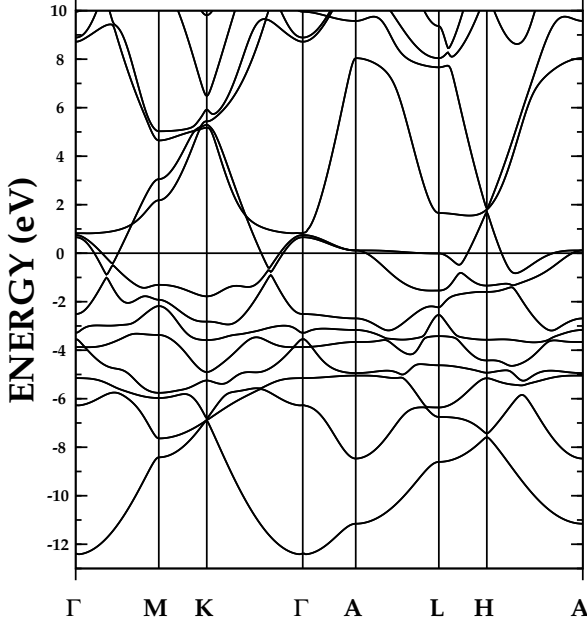


FIG. 2.  $\text{AuB}_2$  band structures along high symmetry lines. Overall features are similar to those of  $\text{AgB}_2$

functions are adopted up to  $l = 3$  for Ag and Au sites and  $l = 2$  for B.

In Fig. 1 and Fig. 2, we have shown band structures of  $\text{AgB}_2$  and  $\text{AuB}_2$ , respectively, along high symmetry lines in the BZ. It is clear that B  $2p$  states near  $E_F$ , corresponding to the in-plane B-B  $p_{x,y}$  bands, are almost dispersionless along  $\Gamma$ –A–L line and yield the hole Fermi surfaces. The effect of the spin-orbit interaction on these bands is minor: the splittings are barely seen in the case of  $\text{AuB}_2$ . Previously, similar band feature producing the cylindrical hole Fermi surface along  $\Gamma$ –A is emphasized in  $\text{MgB}_2$ , as is responsible for superconductivity [8,9]. However, the B  $p\sigma$  bands are flatter in  $\text{AgB}_2$  and  $\text{AuB}_2$  than in  $\text{MgB}_2$ , yielding the higher DOS at  $E_F$  (Fig. 3). The bandwidths of B  $p\sigma$  are less than 5 eV in  $\text{AgB}_2$  and  $\text{AuB}_2$  due to band repulsion between Ag  $4d$  (Au  $5d$ ) and B  $2p$  as is evident along A–L line. Whereas they are as much as 9 eV in  $\text{MgB}_2$  (Fig. 4). The band repulsion drives the B  $2p\sigma$  states to pile up at  $E_F$ .

The calculated DOS's at  $E_F$ ,  $N(0)$ , in various systems are summarized in Table I. We have found that they are about 1.6 and 2.2 times larger in  $\text{AgB}_2$  and  $\text{AuB}_2$  with  $N(0) = 0.557$  and 0.768 states/(eV, spin) than  $N(0) = 0.356$  states/(eV, spin) in  $\text{MgB}_2$ . In addition, the B  $2p$  contributions to the total DOS at  $E_F$  are  $\tilde{N}_B(0) \simeq 0.6$  in all cases. The total and atomic site projected DOS's in Fig. 3 also reflects these features, in which B atoms dominantly contribute to the DOS at  $E_F$ .

Employing the McMillan's empirical formula for  $T_c$  [27],

$$T_c = \frac{\Theta_D}{1.45} \exp \left[ \frac{-1.04(1 + \lambda)}{\lambda - (1 + 0.62\lambda)\mu^*} \right], \quad (1)$$

we have estimated the transition temperatures with the Coulomb pseudopotential parameter of  $\mu^* = 0.1$  and the

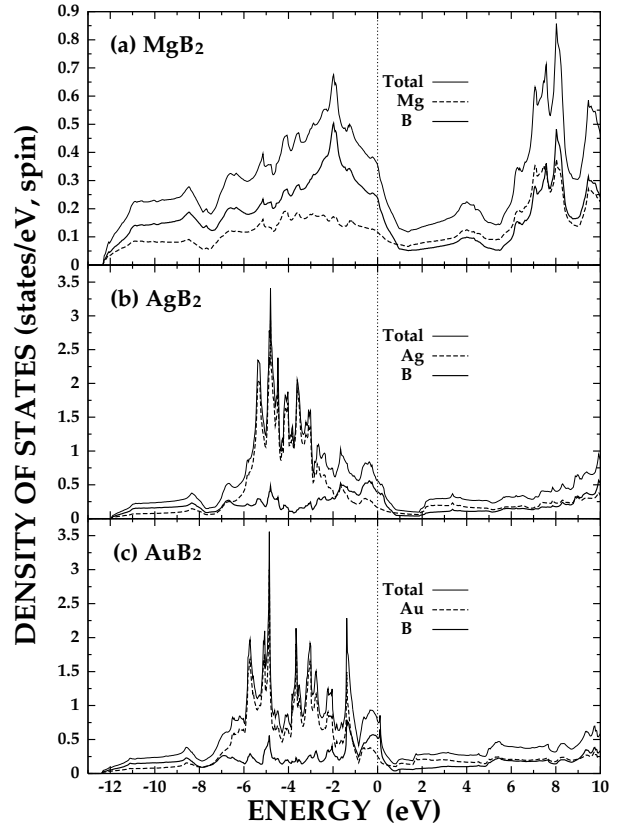


FIG. 3. The atomic site projected DOS in (a)  $\text{MgB}_2$ , (b)  $\text{AgB}_2$ , and (c)  $\text{AuB}_2$ . For the B DOS, two B atomic contributions are summed. In all cases, the B  $2p$  DOS is dominant at  $E_F$ .

the experimental Debye temperature of  $\Theta_D \sim 700$  K [4,6]. We consider the superconducting properties within the framework of the simple rigid-ion approximation [28]. Calculation of  $\eta_\alpha = N(0)\langle I_\alpha^2 \rangle$ , where  $\langle I_\alpha^2 \rangle$  is the average electron-ion interaction matrix element for the  $\alpha$  atom in the unit cell, yields  $\eta_\alpha = 0.03$  and  $1.87$  eV/ $\text{\AA}^2$  for  $\alpha = \text{Mg}$  and B atoms, respectively. Note that the contribution from B atom is dominating. Then the electron-phonon coupling constant,  $\lambda = \sum_\alpha \eta_\alpha / M_\alpha \langle \omega^2 \rangle$ , is evaluated to be  $\lambda = 0.79$ . Here  $M_\alpha$  is an ionic mass and  $\langle \omega^2 \rangle$  is the average phonon frequency approximated by  $\langle \omega^2 \rangle \simeq \Theta_D^2/2$ .

First of all, we would like to point out that our estimated values of  $\lambda = 0.79$  and the corresponding  $T_c^{\text{cal}} = 27$  K for  $\text{MgB}_2$  are in good agreement with other theoretical [8,9,29] and experimental values. In a similar way, we have also estimated superconducting properties of  $\text{AgB}_2$  and  $\text{AuB}_2$ , assuming that the phonon frequencies are of the same order as that in  $\text{MgB}_2$ . It is a plausible approximation because the ionic radii of Ag and Au are similar to that of Mg [30] and the relevant phonon mode is the in-plane B bond stretching mode. Remarkably, as shown in Table I, we have obtained almost twice larger  $\eta_B$ 's for  $\text{AgB}_2$  and  $\text{AuB}_2$  than that for  $\text{MgB}_2$ , and so the electron-phonon coupling constant values are  $\lambda = 1.35$  and  $1.65$  for  $\text{AgB}_2$  and  $\text{AuB}_2$ , respectively. With these values, we have estimated the transition temperatures of  $T_c^{\text{cal}} = 59$  K

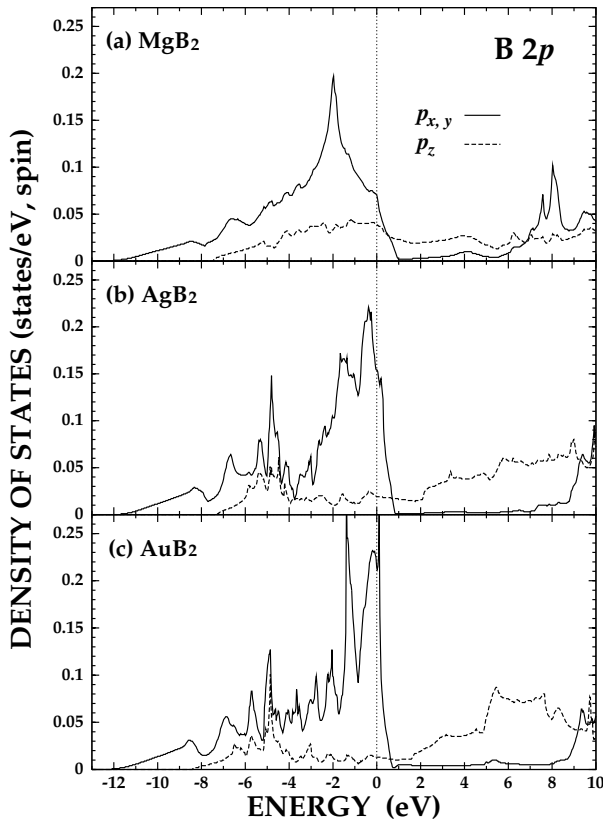


FIG. 4. Directionally decomposed B  $2p$  DOS in (a)  $\text{MgB}_2$ , (b)  $\text{AgB}_2$ , and (c)  $\text{AuB}_2$ . In going from  $\text{MgB}_2$  to  $\text{AgB}_2$  and  $\text{AuB}_2$ , the B  $2p_{x,y}\sigma$  DOS at  $E_F$  becomes larger.

for  $\text{AgB}_2$  and 72 K for  $\text{AuB}_2$ . They are 2  $\sim$  3 times larger than that in  $\text{MgB}_2$ , and even comparable to those in high temperature cuprate superconductors.

It may be difficult to find right condition of synthesizing stoichiometric  $\text{AgB}_2$  and  $\text{AuB}_2$  compounds. In such a case, first attempt would be to synthesize hole doped materials like  $\text{Mg}_{1-x}\text{Ag}_x\text{B}_2$  and  $\text{Mg}_{1-x}\text{Au}_x\text{B}_2$  or to grow them in films. At least, hole doped samples could be obtained, considering that  $\text{Mg}_{1-x}\text{Li}_x\text{B}_2$  has been already tested including  $x = 1.0$  [24]. On the other hand, it was reported that Cu substitution in  $\text{MgB}_2$  produces  $\text{MgCu}_2$  phase rather than  $\text{CuB}_2$  [25]. This unfortunate occasion is likely to arise because the ionic radius difference between Cu and Mg is large, and hence Cu prefers to sit at the B site [31]. On the other hand, Ag and Au share similar ionic radius with Mg, and so it is expected that these elements will be in better situation than the Li and Cu cases. In addition, one may use  $\text{Mg}_{1-x}\text{Ag}_x\text{B}_2$  and  $\text{Mg}_{1-x}\text{Au}_x\text{B}_2$  to examine the existing theory which sets the upper limit of the transition temperature in the phonon-mediated BCS mechanism superconductor as  $T_c \lesssim 40$  K. If the proposed noble metal  $\text{HT}_c\text{BS}$ 's are realized, it is expected that, besides high  $T_c$ , they will also have the enhanced hole concentration of  $n_h = 0.120$  and  $0.128$  holes/B in comparison with  $n_h = 0.06$  holes/B in  $\text{MgB}_2$  (Table I and Fig. 4). These things will serve more favorably for technological applications.

TABLE I. The DOS's at  $E_F$ ,  $N(0)$  and  $N_B(0)$ , are in unit of states/( $\text{MB}_2$ , eV, spin) and states/(B  $2p$ , eV, spin), respectively.  $\tilde{N}_B(0)$  given by the ratio of  $2N_B(0)/N(0)$  is B  $2p$  contribution to the total DOS at  $E_F$ .  $n_h$  denotes the number of holes in B-B  $p\sigma$  band per B atom.  $\eta_B$  is the McMillan-Hopfield parameter for B atom and  $\lambda$  is the electron-phonon coupling constant. The transition temperature  $T_c^{\text{cal}}$  is estimated by using the McMillan's formula with  $\mu^* = 0.1$  and  $\Theta_D = 700$  K. For  $\text{MgB}_2$ , present results are consistent with other calculations.

	$N(0)$	$N_B(0)$	$\tilde{N}_B(0)$	$n_h$	$\eta_B$	$\lambda$	$T_c^{\text{cal}}$ (K)
$\text{MgB}_2$	0.356	0.109	0.612	0.062	1.87	0.79	27
$\text{CuB}_2^a$	0.710	0.195	0.550	0.088	3.50	1.48	65
$\text{AgB}_2$	0.557	0.173	0.628	0.128	3.17	1.35	59
$\text{AuB}_2$	0.768	0.225	0.586	0.120	3.88	1.65	72

<sup>a</sup> Reference [31]

In conclusion, we have performed band structure calculations for  $\text{AgB}_2$  and  $\text{AuB}_2$  to search for new  $\text{HT}_c\text{BS}$ . These are predicted to be very promising materials to meet the purpose, and thus the material synthesis and experimental measurements are encouraged.

Acknowledgements— This work was supported by KOSEF through eSSC at POSTECH and in part by the BK21 Project.

- [1] J. Nagamatsu, N. Nakagawa, T. Muranaka, Y. Zenitani, and J. Akimitsu, *Nature* **410**, 63 (2001).
- [2] T. Takahashi, T. Sato, S. Souma, T. Muranaka, and J. Akimitsu, *Phys. Rev. Lett.* **86**, 4915 (2001).
- [3] G. Rubio-Bollinger, H. Suderow, and S. Vieira, *Phys. Rev. Lett.* **86**, 5582 (2001).
- [4] S. L. Bud'ko, *et al.*, *Phys. Rev. Lett.* **86**, 1877 (2001).
- [5] D. G. Hinks, H. Claus, and J. D. Jorgensen, *Nature* **411**, 457 (2001).
- [6] R. Osborn, E. A. Goremychkin, A. I. Kolesnikov, and D. G. Hinks, *Phys. Rev. Lett.* **87**, 017005 (2001).
- [7] J. S. Slusky, *et al.*, *Nature* **410**, 343 (2001).
- [8] J. M. An and W. E. Pickett, *Phys. Rev. Lett.* **86**, 4366 (2001).
- [9] J. Kortus, I. I. Mazin, K. D. Belashchenko, V. P. Antropov, and L. L. Boyer, *Phys. Rev. Lett.* **86**, 4656 (2001).
- [10] W. N. Kang, H.-J. Kim, E.-M. Choi, C. U. Jung, and S.-I. Lee, *Science* **292**, 1521 (2001).
- [11] P. C. Canfield, *et al.*, *Phys. Rev. Lett.* **86**, 2423 (2001).
- [12] C. B. Eom, *et al.*, *Nature* **411**, 558 (2001).
- [13] Y. Bugoslavsky, *et al.*, *Nature* **411**, 561 (2001).
- [14] S. Jin, H. Mavoori, C. Bower, and R. B. van Dover, *Nature* **411**, 563 (2001).
- [15] A. S. Cooper, E. Corenzwit, L. D. Longinotti, B. T. Matthias, and W. H. Zachariasen, *Proc. Natl. Acad. Sci. USA* **67**, 313 (1970).
- [16] D. Kaczorowski, A. J. Zaleski, O. J. Żogal, and J. Klamut, *cond-mat/0103571*.
- [17] V. A. Gasparov, N. S. Sidorov, I. I. Zver'kova, and M. P. Kulakov, *condmat/0104323*.

- [18] P. P. Singh, cond-mat/0104580.
- [19] H. Rosner, *et al.*, cond-mat/0106092.
- [20] G. Satta, G. Profeta, F. Bernadini, A. Continenza, and S. Massidda, cond-mat/0102358.
- [21] N. I. Medvedeva, A. L. Ivanovskii, J. E. Medvedeva, and A. J. Freeman, Phys. Rev. B **64**, 020502(R) (2001).
- [22] P. Ravindran, P. Vajeeston, R. Vidya, A. Kjekshus, and H. Fjellvåg, cond-mat/0104253.
- [23] N. I. Medvedeva, A. L. Ivanovskii, J. E. Medvedeva, A. J. Freeman, and D. L. Novikov, cond-mat/0104346.
- [24] Y. G. Zhao, *et al.*, cond-mat/0103077.
- [25] Y. Moritomo and Sh. Xu, cond-mat/0104568.
- [26] S. J. Youn (unpublished, 2001). The equilibrium lattice constants are determined by the total energy calculations using the full-potential linearized-augmented plane wave (FLAPW) band method (M. Weinert, E. Wimmer, and A. J. Freeman, Phys. Rev. B **26**, 4571 (1982); H. J. F. Jansen and A. J. Freeman, Phys. Rev. B **26**, 4571 (1982)).
- [27] W. L. McMillan, Phys. Rev. **167**, 331 (1968).
- [28] G. D. Gaspari and B. L. Gyorffy, Phys. Lett. **28**, 801 (1972).
- [29] Y. Kong, O. V. Dolgov, O. Jepsen, and O. K. Andersen, Phys. Rev. B **64** 020501(R) (2001).
- [30] C. Kittel, *Introduction to Solid States Physics*, (John Wiley & Sons, New York, 1996), 7th ed. Chap. 3.
- [31] Although CuB<sub>2</sub> phase was not produced experimentally, electronic structure calculation is performed for  $a = 2.96 \text{ \AA}$  and  $c = 3.25 \text{ \AA}$ , which are optimized values by using the FLAPW method. The transition temperature ignoring the Cu  $d$ - $f$  channel in the rigid-ion approximation is estimated to be  $T_c = 65 \text{ K}$ .